THE JOURNAL OF PHYSICAL CHEMISTRY Letters

Letter

Cite This: J. Phys. Chem. Lett. 2019, 10, 7498−7504

pubs.acs.org/JPCL

Steric Interactions Impact Vibronic and Vibrational Coherences in Perylenediimide Cyclophanes

Jonathan D. Schultz, Adam F. Coleman, Aritra Mandal, Jae Yoon Shin, Mark A. Ratner, Ryan M. Young,* and Michael R. Wasielewski*

Department of Chemistry and Institute for Sustainability and Energy at Northwestern, Northwestern University, Evanston, Illinois 60208-3113, United States

Supporting Information

ABSTRACT: Designing molecular systems that exploit vibronic coherence to improve light harvesting efficiencies relies on understanding how interchromophoric interactions, such as van der Waals forces and dipolar coupling, influence these coherences in multichromophoric arrays. However, disentangling these interactions requires studies of molecular systems with tunable structural relationships. Here, we use a combination of two-dimensional electronic spectroscopy and femtosecond stimulated Raman spectroscopy to investigate the role of steric hindrance between chromophores in driving changes to vibronic and vibrational coherences in a series of substituted perylenediimide (PDI) cyclophane dimers. We report significant differences in the frequency power spectra from the cyclophane dimers versus the corresponding monomer reference. We attribute these differences to distortion of the PDI cores from steric interactions between the substituents. These results highlight the importance of considering structural changes when rationalizing vibronic coupling in multichromophoric systems.

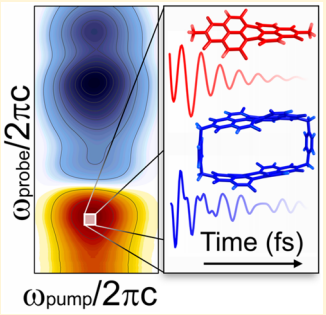

The function of quantum coherence in excitation energy transfer has been a topic of interest to biologists, chemists, and physicists for decades.[1−3] Recent developments in multidimensional optical spectroscopy[4] have highlighted the importance of vibronic coherence, i.e., phase-related superpositions with mixed nuclear and electronic character, in natural photosynthetic complexes. Studies suggest these coherences may enhance both the rate and efficiency of energy and charge transfer in multichromophoric systems.[3,5−12] While coherence phenomena have been examined in several chromophores,[13−21] relatively few studies have focused on well-defined structures having a small number of chromophores, such as dimers and trimers, from which design principles regarding larger light harvesting arrays can be developed.[15,16]

Small chromophore assemblies having synthetically tunable structures allow for extracting maximal insight into the factors that influence vibronic coherences.[11,12,15,16,22] Through this bottom-up approach, researchers have elucidated the role of energy level ordering[12,16] and conformational disorder[16,22] in controlling the degree of electronic-vibrational coupling. An additional important factor to address is van der Waals forces between neighboring chromophores. Depending on the orientation and packing of the chromophores, structural distortions resulting from steric interactions may strongly impact vibronic couplings through changes in Franck−Condon (FC) factors and/or broken molecular symmetry.[23] In order to rationalize these effects in light-harvesting arrays, we must first build a better fundamental understanding by exploring model systems with precise control over interchromophoric interactions.

Perylenediimide (PDI) is a particularly interesting organic chromophore from this perspective[24] because it is synthetically tunable,[25] which facilitates its tailoring to a wide variety of applications such as highly efficient fluorescence,[26,27] photoinduced energy[28] and electron transfer,[29] and singlet fission.[30] PDI derivatives have been utilized in organic electronics,[31,32] artificial photosynthesis,[33] and organic photovoltaic devices.[34] We wish to use the covalent control afforded by PDI cyclophane dimers[35] (Scheme 1) to investigate how van der Waals forces influence vibronic coherences. In particular, cyclophanes incorporating 1,6,7,12-tetrakis(4-*t*-butylphenoxy)-perylene-3,4:9,10-bis(dicarboximide) chromophores allow us to precisely fix the interchromophoric distance using different linking groups. Inclusion of such bulky bay-substituents has been shown to induce twisting in the monomeric PDI core.[35−37] Different degrees of steric interactions between the 4-*t*-butylphenoxy groups in the cyclophanes may alter the extent of twisting in the PDI cores, which allows us to examine how substituent interactions and resultant differences in core structure affect vibronic and/or vibrational coherences. Here we report significant differences in the relative amplitudes of signal modulations stemming from excited- and ground-state wavepackets in the cyclophane dimers versus the corresponding monomer reference. These coherences may play an

Received: October 3, 2019
Accepted: November 15, 2019
Published: November 15, 2019

DOI: 10.1021/acs.jpclett.9b02923
J. Phys. Chem. Lett. 2019, 10, 7498−7504

Scheme 1. Molecular Structures for the Compounds in This Study[a]

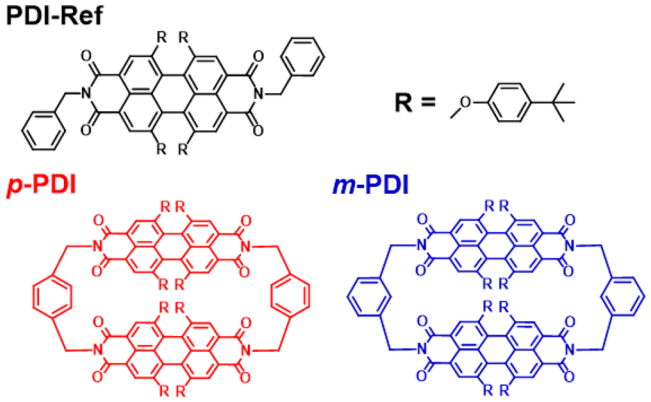

[a]PDI-Ref, *p*-PDI, and *m*-PDI represent the PDI monomer, *para*-connected, and *meta*-connected cyclophanes, respectively.

important role in symmetry-breaking charge separation[29] and singlet fission[30] involving PDI cyclophanes, processes that are both important for photodriven charge separation leading to energy storage.

The cyclophanes reported here are composed of monomeric 4-*t*-butylphenoxy (bay) substituted PDI units covalently bound via para (*p*-PDI) or meta (*m*-PDI) connections to benzyl group linkers. Molecular structures for *p*-PDI, *m*-PDI, and the reference compound, PDI-ref, are provided in Scheme 1. The synthesis details and characterization of the intermediates and final products are provided in the Supporting Information (SI). Normalized visible electronic absorption spectra for PDI-ref, *p*-PDI, and *m*-PDI dissolved in THF at room temperature are shown in Figure 1. PDI-ref exhibits a prominent vibronic progression of ~1280 cm^{-1} with absorption maxima near 17 600 and 18 890 cm^{-1} (568 and 530 nm, respectively). The absorption spectra of *p*-PDI and *m*-PDI exhibit similar vibronic progressions, but with an increasing absorption near the 0−1 vibronic band relative to that of the 0−0 transition. This altered ratio of the vibronic bands is well described by positive dipolar coupling between the cofacial PDI moieties (H-aggregation),[23,38] which is further reflected by the blueshift of the absorption maxima in *m*-PDI relative to PDI-ref. Simulation of the linear absorption spectra with the Holstein Hamiltonian (Figure S5) yields dipolar couplings of ~180 and ~270 cm^{-1} for *p*-PDI and *m*-PDI, respectively, in agreement with previous work on similar systems.[35] This is thus the energy regime we are interested in investigating for vibronic coupling phenomena.

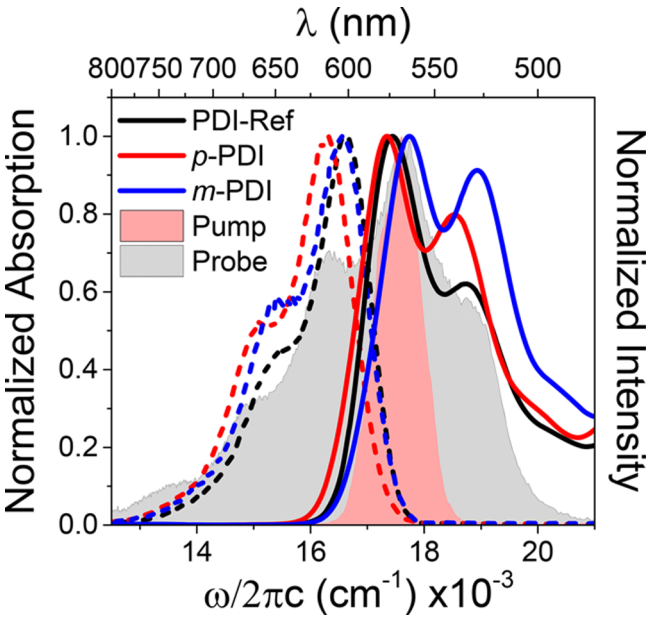

Figure 1. Normalized steady-state absorption (solid) and emission (dashed) spectra of PDI-ref, *p*-PDI, and *m*-PDI obtained in THF at room temperature. Pump and probe pulses for the 2DES measurements are superimposed.

We characterize the coherences in these systems with a combination of two-dimensional electronic spectroscopy (2DES) and femtosecond stimulated Raman spectroscopy (FSRS) in order to disentangle vibronic from vibrational coherences. 2DES is a powerful third-order nonlinear spectroscopic technique which produces optical spectra with frequency resolution in both the pump and probe pulse dimensions.[4,39,40] A rich understanding of the Franck−Condon envelope of a molecule can be obtained through this technique because the short time duration pump pulses can generate coherent wavepackets composed of FC-active vibrations on both the ground and excited states.[1,3,11,41] Such wavepackets manifest themselves as amplitude oscillations of relevant spectral features as a function of the time between the second pump pulse and the probe.[41] In contrast to 2DES, by using a narrowband resonant Raman pump, FSRS is capable of generating and probing purely vibrational coherences on the molecular ground or excited state surface, depending on the resonance of the Raman pump.[42,43] FSRS therefore provides a complementary method of unraveling the contributions of electronic and vibrational character to the coherences observed via 2DES.

2DES spectra were collected following $S_1 \leftarrow S_0$ excitation of PDI-ref, *p*-PDI, and *m*-PDI. Experimental details are provided in the SI. Spectra of the three compounds at a waiting time delay of 150 fs are shown in Figure 2. Each system displays negative ground-state bleach (GSB) features near ω_{pump} (ω_1) = ω_{probe} (ω_3) = 17 500 cm^{-1} with a higher-energy vibronic transition ~1300 cm^{-1} above the diagonal in the probe dimension. A negative stimulated emission (SE) band can be observed ~1300 cm^{-1} below the diagonal. Positive excited-state absorption (ESA) features are observed near (ω_1 = 17 500 cm^{-1}, ω_3 = 14 000 cm^{-1}) and (ω_1 = 17 500 cm^{-1}, ω_3 = 10 500 cm^{-1}), which correspond to $S_n \leftarrow S_1$ transitions.

The nature of the coherences observed in 2DES experiments has been widely debated.[1,3,7,11] The spectral region accessible by our pump is particularly relevant to investigate considering these frequencies are on the energetic order of the exciton coupling in the dimer systems. Thus, vibrations in this frequency region may mix strongly with the electronic degrees of freedom.[7] To address the effects of interchromophoric steric interactions on the nature of such coherences in these PDI systems, we separated the oscillatory signals from population dynamics in the 2DES data by fitting and subtracting the population kinetics at each (ω_1, ω_3) coordinate as a function of the waiting time. Representative time traces and corresponding population fits for PDI-ref, *p*-PDI, and *m*-PDI are shown in Figure 3A−C, respectively.

We examined the fast Fourier transform (FFT) of the isolated traces at each (ω_1, ω_3) position to extract frequency-

DOI: 10.1021/acs.jpclett.9b02923
J. Phys. Chem. Lett. 2019, 10, 7498−7504

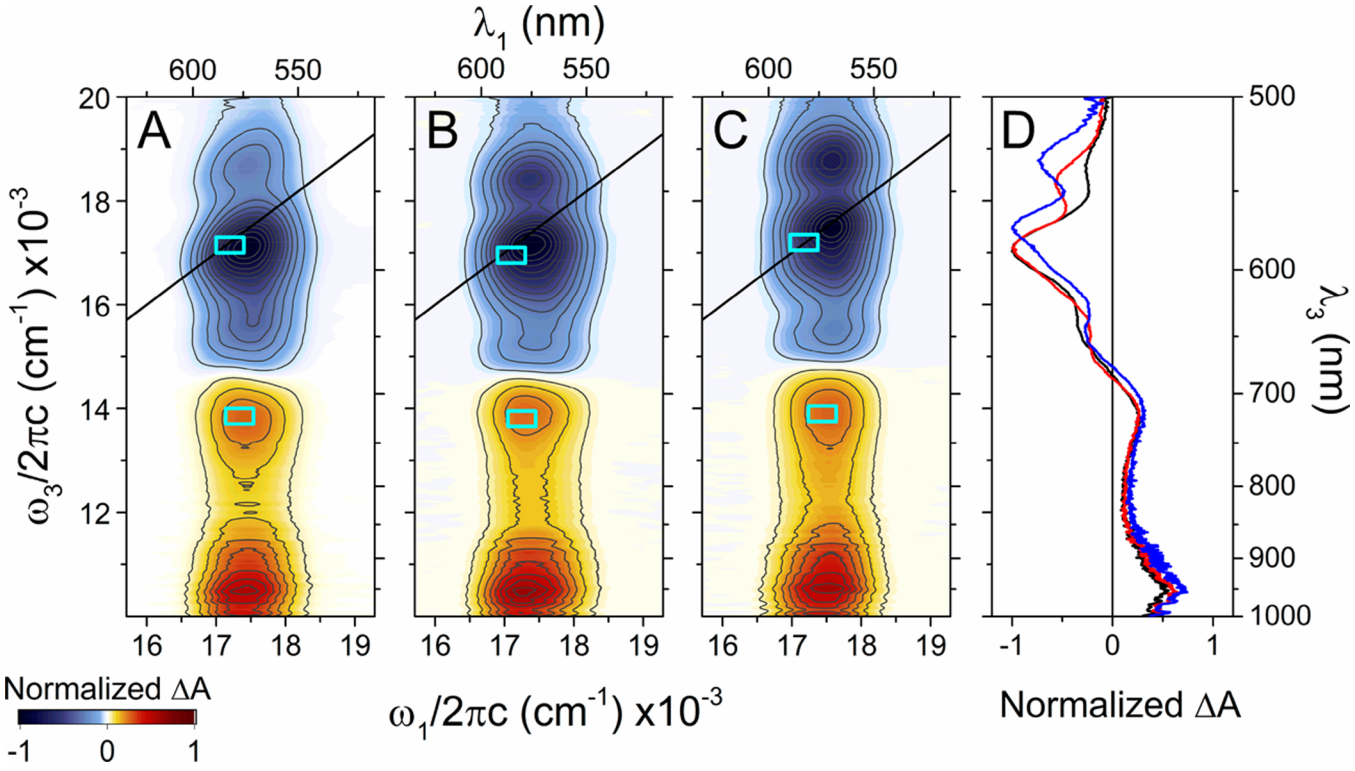

Figure 2. Absorptive 2DES spectra at a waiting time of 150 fs for (A) PDI-ref, (B) *p*-PDI, and (C) *m*-PDI obtained in THF at room temperature. Each spectrum is normalized to the maximum absolute change in absorption. Cyan rectangles indicate the approximate regions over which the coherence analysis was performed. (D) Corresponding transient absorption spectra for PDI-ref (black), *p*-PDI (red), and *m*-PDI (blue).

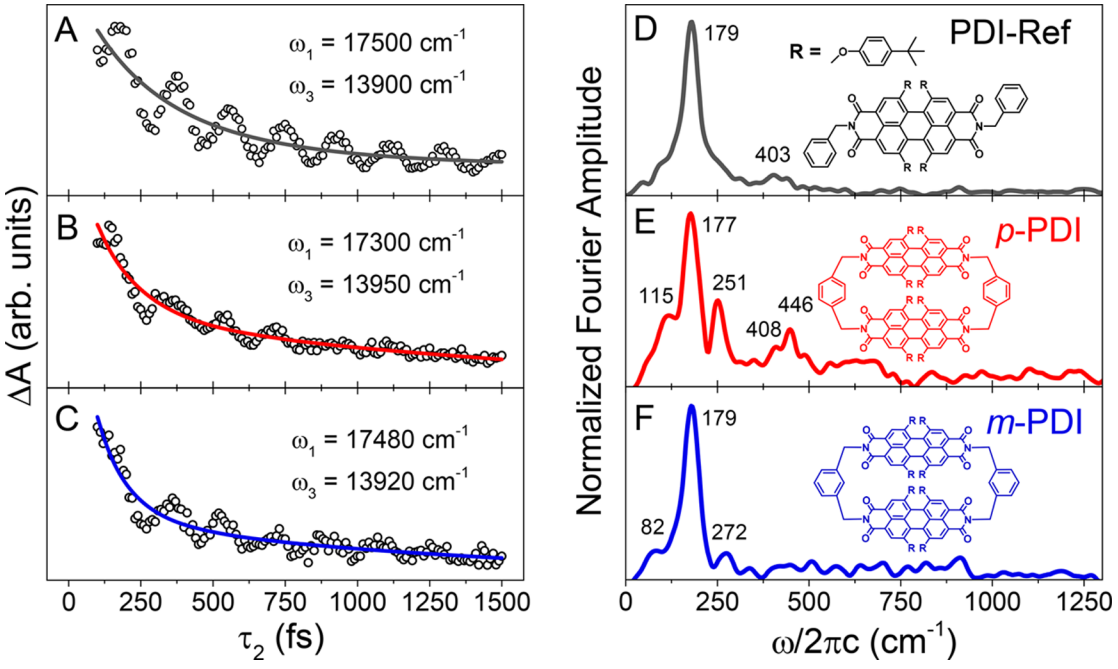

Figure 3. Time-domain data (hollow circles) from the real part of the 2DES signal and exponential fits (solid lines) integrated over a 30 × 30 cm^{-1} region near the specified coordinates for (A) PDI-ref, (B) *p*-PDI, and (C) *m*-PDI. Frobenius norms calculated in the frequency domain across a 300 × 400 cm^{-1} region on the higher energy $S_n \leftarrow S_1$ ESA feature for (D) PDI-ref, (E) *p*-PDI, and (F) *m*-PDI. Replicate and control traces are available in the SI.

domain information regarding the oscillations present in the PDI-ref, *p*-PDI, and *m*-PDI 2DES data. Frobenius norms of the frequency-domain signals across a limited spectral region were used to improve the signal-to-noise ratio and better sample the oscillations associated with the specific optical transition; these norms were chosen to be centered near the maximum of the oscillatory beating amplitude (cyan rectangles in Figures 2 and S18). We first turn our attention to excited-state oscillatory signatures in these data, as these are most relevant to application in coherent energy transport.[10] While such signals

DOI: 10.1021/acs.jpclett.9b02923
J. Phys. Chem. Lett. 2019, 10, 7498−7504

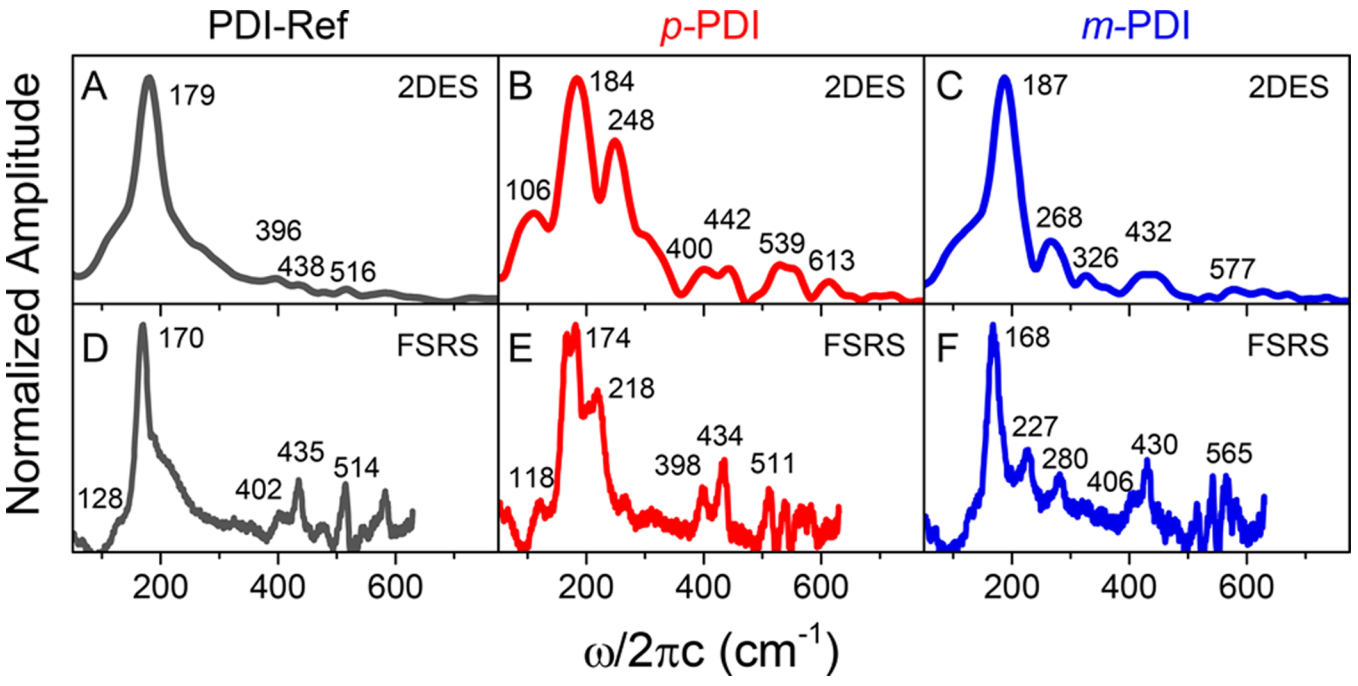

Figure 4. Normalized ground-state 2DES and FSRS spectra for (A and D) PDI-ref, (B and E) *p*-PDI, and (C and F) *m*-PDI, respectively, in THF at room temperature. Replicate and control traces are available in the SI.

can be deconvoluted from those associated with coherences on the ground state in the GSB region of the 2D spectrum,[44,45] the wide spectral coverage in the probe dimension here permits resolution of purely ESA features, which can only exhibit excited-state coherences. Normalized power spectra of the oscillations integrated across the higher-energy ESA feature for PDI-ref, *p*-PDI, and *m*-PDI are shown in Figure 3D−F, respectively. In the excited-state power spectrum for PDI-ref, we observe peaks at 179 and 403 cm^{-1}. In contrast, the spectrum of *p*-PDI contains additional peaks at 115, 251, and 446 cm^{-1} and a clear increase in the relative intensity of the 408 cm^{-1} mode. The oscillations below 300 cm^{-1} observed in *p*-PDI remain prominent in *m*-PDI, where the interchromophoric distance is decreased, but at significantly lower intensities relative to the strongest peak near 179 cm^{-1}. A peak near 400 cm^{-1} is observed in some *m*-PDI experiments (Figures S11 and S16F), but also at lower relative intensity compared to that in the *p*-PDI power spectrum.

Several factors can contribute to the differences between the power spectra for PDI-ref, *p*-PDI, and *m*-PDI. The presence of an additional coherence in a dimer system compared to the monomer could imply the oscillation originates from a superposition of two excitonic states induced by dipolar coupling.[11] However, such purely electronic coherences are reported to dephase on the order of tens of femtoseconds.[11,46,47] Considering these measurements were conducted in room temperature solutions and data prior to 100 fs are neglected, the features observed in *p*-PDI and *m*-PDI are most likely not purely excitonic in origin. While the coherences are purely vibrational in PDI-ref, those observed in the dimers are likely vibronic in nature since both the linear absorption and 2DES spectra indicate the presence of Frenkel excitons. Thus, one explanation for the differences between Figure 3D−F could be varying degrees of transition dipole coupling in the dimers, which will alter the degree of interaction between excitons and underdamped vibrational modes.[7,11,48] Studies have predicted[7,48] and shown[16] amplitude enhancement of vibronic coherences when excitonic splitting yields bright vibronic states not present in the monomer.

While this enhancement has received much attention in recent literature,[7,16,48] it is important to note that structural deformations of the monomer units in the cyclophanes could also account for the observed differences in the power spectra. As discussed above, it is known that bay substituents in PDI molecules can induce twisting in the core.[37] Steric interactions between the substituents in the dimers here could result in changes to the degree of core twisting in relation to the isolated monomer; this effect could be exacerbated at smaller chromophore spacings. Such structural deformations may alter the displacement between the ground- and excited-state potential energy minima and thus yield different sets of FC factors for each system, thereby leading to different signal amplitudes from vibronic coherences.

Deconvoluting the influence of excitonic splitting versus steric hindrance in these results requires evaluation of the origin state (ground or excited) of the coherence. Isolating purely ground-state signals from those on the excited state surface is known to be difficult in room-temperature 2DES.[44,45] However, the ultrafast Stokes shift observed in these systems (Figure S19D) results in transient separation of the these signals in the probe frequency dimension, with ground- and excited-state oscillations occurring primarily near and below the diagonal in the 2D maps, respectively. Figure 4A−C shows power spectra integrated at frequencies near the diagonal, thus reflecting primarily ground-state coherences for PDI-ref, *p*-PDI, and *m*-PDI. However, some excited-state contribution from SE pathways cannot be explicitly ruled out. Similar to the purely excited-state results, a dominant oscillation frequency (~179 cm^{-1}) with potential shoulders is observed for PDI-ref. In comparison, peaks near 106, 248, 400, 442, 539, and 613 cm^{-1} grow in relative intensity in the *p*-PDI power spectrum.

DOI: 10.1021/acs.jpclett.9b02923
J. Phys. Chem. Lett. 2019, 10, 7498−7504

Most of these modes are apparent in the spectrum for *m*-PDI, but with significant reduction in relative intensity.

It is important to note here that some ground-state vibrational coherence signals will also be altered substantially by vibronic coupling due to intensity borrowing.[7,48] Conversely, signals which do not involve resonance with both excitonic states will not undergo this signal amplification mechanism and will be primarily sensitive to alterations in FC factors between the compounds.[7] The tendency for excited- and ground-state oscillatory signals to overlap in 2DES complicates exploitation of this notion, but FSRS offers a complementary method of isolating such a signal. Thus, we examined pure ground-state coherence signatures from PDI-ref, *p*-PDI, and *m*-PDI using FSRS. By using a Raman pump preresonant with the $S_1 \leftarrow S_0$ absorption band, we only observe those coherences resonantly enhanced by the lower-energy exciton state in the dimers.

Figure 4D−F shows Stokes FSRS spectra for the PDI compounds. PDI-ref exhibits a strong mode at 170 cm^{-1} and numerous peaks between 400 and 600 cm^{-1}. The 170 cm^{-1} peak is accompanied by weak shoulders. In comparison, the FSRS spectrum of *p*-PDI shows two additional intense peaks at 118 and 218 cm^{-1} and slightly increased relative intensity of the peaks at 398 and 434 cm^{-1}. We also observe other peaks between 500 and 600 cm^{-1}, but they do not show increased relative intensity compared to those observed for PDI-ref. The spectrum for *m*-PDI exhibits similar peaks at 227, 406, and 430 cm^{-1}. The relative amplitude of the former is significantly reduced when compared to the corresponding peak in the *p*-PDI spectrum, while the relative intensities of the latter two modes are only slightly reduced.

The ground-state FSRS results corroborate many of the peak trends noted both from Figures 3D−F and 4A−C. As discussed above, the primary pathway leading to FSRS gain in a ground-state experiment should be minimally affected by the vibronic enhancement mechanism that has been discussed in the context of time-domain oscillations in 2DES.[7,48] Thus, the Raman data imply the amplitude differences in the ground-state 2DES power spectra between PDI-ref, *p*-PDI, and *m*-PDI can be described predominantly by changes to FC factors and not intensity borrowing from coherent interaction between dimer exciton states and near-resonant vibrational states. Though peak amplitudes in the excited-state power spectra in Figure 3D−F additionally rely on FC factors between the S_1 and a higher-lying excited state, the similarity between the excited- and ground-state 2DES trends suggests that the excited-state coherences are also impacted primarily by changes to FC factors apart from vibronic enhancement. These claims are further supported by an additional 2DES experiment we conducted with the pump center moved ∼500 cm^{-1} higher in energy, where the results show nearly identical trends to the ones we presented here despite having different resonance conditions with the low frequency vibrational and/or vibronic states (Figure S16). Furthermore, excited-state FSRS spectra for each compound corroborate our conclusions with similar trends present to those of the ground-state (Figure S21).

While the prominent vibrations exhibited by unsubstituted PDI variants in previous literature[49,50] are characterized by in-plane ring distortion, inclusion of the 4-*t*-butylphenoxy substituents in the systems here leads to significant twisting of the PDI core,[35−37,51] thus heavily altering the nature of the vibrations in the low frequency region of the Raman spectrum. Both dimerization and decreasing interchromophoric spacing by changing the benzyl linkage introduces extra steric hindrance between the substituents and thus likely alters the degree of core twisting. Considering that the low frequency vibrations in these systems primarily involve motions of the PDI core nuclei, as revealed by DFT normal-mode analysis on PDI-ref (Figure S22), this structural strain may result in a combination of altered FC factors and the presence of new normal modes. Such an effect accounts for the differences observed in both the 2DES power and FSRS spectra for PDI-ref, *p*-PDI, and *m*-PDI without invoking the vibronic enhancement mechanism. Furthermore, it is worth noting that similar trends in the relative intensity of Raman-active modes in cyclophane dimers as a function of decreasing $\pi-\pi$ distance have been observed previously,[52] which suggests that this result may be general to systems of closely spaced chromophores.

Here we have shown a significant dependence of the vibronic and vibrational coherences in PDI cyclophanes upon interchromophoric interactions. Through comparison of the power spectra obtained via time-domain 2DES signal modulations to FSRS measurements and DFT calculations, we determined this dependence is of structural origin. While vibronic enhancement is potentially present in some of the observed oscillations, our results suggest this mechanism cannot fully account for the trends. For PDI systems specifically, our results indicate particular chromophore arrangements may be ideal for strong prevalence of certain coherences. Furthermore, these results illustrate the sensitivity of vibronic and vibrational coherences to van der Waals forces between neighboring chromophores. Such knowledge is critical for understanding how vibronic coherences may be exploited for efficient energy transfer in synthetic light-harvesting arrays.

■ ASSOCIATED CONTENT

Supporting Information

The Supporting Information is available free of charge at https://pubs.acs.org/doi/10.1021/acs.jpclett.9b02923.

Synthetic and spectroscopic methods, additional 2DES and FSRS spectra, and computational outputs (PDF)

■ AUTHOR INFORMATION

Corresponding Authors

*E-mail: m-wasielewski@northwestern.edu.

*E-mail: ryan.young@northwestern.edu.

ORCID

Jonathan D. Schultz: 0000-0002-3386-5460

Aritra Mandal: 0000-0002-8680-3730

Ryan M. Young: 0000-0002-5108-0261

Michael R. Wasielewski: 0000-0003-2920-5440

Notes

The authors declare no competing financial interest.

■ ACKNOWLEDGMENTS

We thank Drs. Brian Phelan and Pyosang Kim for useful spectroscopic discussions. This work was supported by the National Science Foundation under grant number DMR-1710104. This material is based upon work supported by the National Science Foundation Graduate Research Fellowship Program under Grant No. DGE-1842165. Any opinions, findings, and conclusions or recommendations expressed in

DOI: 10.1021/acs.jpclett.9b02923
J. Phys. Chem. Lett. 2019, 10, 7498−7504

this material are those of the author(s) and do not necessarily reflect the views of the National Science Foundation.

REFERENCES

(1) Engel, G. S.; Calhoun, T. R.; Read, E. L.; Ahn, T. K.; Mancal, T.; Cheng, Y. C.; Blankenship, R. E.; Fleming, G. R. Evidence for wavelike energy transfer through quantum coherence in photosynthetic systems. *Nature* **2007**, *446*, 782−786.

(2) Savikhin, S.; Buck, D. R.; Struve, W. S. Oscillating anisotropies in a bacteriochlorophyll protein: Evidence for quantum beating between exciton levels. *Chem. Phys.* **1997**, *223*, 303−312.

(3) Fuller, F. D.; Pan, J.; Gelzinis, A.; Butkus, V.; Senlik, S. S.; Wilcox, D. E.; Yocum, C. F.; Valkunas, L.; Abramavicius, D.; Ogilvie, J. P. Vibronic coherence in oxygenic photosynthesis. *Nat. Chem.* **2014**, *6*, 706−711.

(4) Jonas, D. M. Two-dimensional femtosecond spectroscopy. *Annu. Rev. Phys. Chem.* **2003**, *54*, 425−463.

(5) Tiwari, V.; Peters, W. K.; Jonas, D. M. Electronic energy transfer through non-adiabatic vibrational-electronic resonance. I. Theory for a dimer. *J. Chem. Phys.* **2017**, *147*, 154308.

(6) Tiwari, V.; Jonas, D. M. Electronic energy transfer through non-adiabatic vibrational-electronic resonance. II. 1D spectra for a dimer. *J. Chem. Phys.* **2018**, *148*, 084308.

(7) Tiwari, V.; Peters, W. K.; Jonas, D. M. Electronic resonance with anticorrelated pigment vibrations drives photosynthetic energy transfer outside the adiabatic framework. *Proc. Natl. Acad. Sci. U. S. A.* **2013**, *110*, 1203−1208.

(8) Womick, J. M.; Moran, A. M. Vibronic Enhancement of Exciton Sizes and Energy Transport in Photosynthetic Complexes. *J. Phys. Chem. B* **2011**, *115*, 1347−1356.

(9) Romero, E.; Novoderezhkin, V. I.; van Grondelle, R. Quantum design of photosynthesis for bio-inspired solar-energy conversion. *Nature* **2017**, *543*, 355−365.

(10) Chenu, A.; Scholes, G. D. Coherence in Energy Transfer and Photosynthesis. *Annu. Rev. Phys. Chem.* **2015**, *66*, 69−96.

(11) Halpin, A.; Johnson, P. J.; Tempelaar, R.; Murphy, R. S.; Knoester, J.; Jansen, T. L.; Miller, R. J. Two-dimensional spectroscopy of a molecular dimer unveils the effects of vibronic coupling on exciton coherences. *Nat. Chem.* **2014**, *6*, 196−201.

(12) Lim, J.; Palecek, D.; Caycedo-Soler, F.; Lincoln, C. N.; Prior, J.; von Berlepsch, H.; Huelga, S. F.; Plenio, M. B.; Zigmantas, D.; Hauer, J. Vibronic origin of long-lived coherence in an artificial molecular light harvester. *Nat. Commun.* **2015**, *6*, 7755.

(13) Scholes, G. D.; Fleming, G. R.; Chen, L. X.; Aspuru-Guzik, A.; Buchleitner, A.; Coker, D. F.; Engel, G. S.; van Grondelle, R.; Ishizaki, A.; Jonas, D. M.; et al. Using coherence to enhance function in chemical and biophysical systems. *Nature* **2017**, *543*, 647−656.

(14) Bredas, J. L.; Sargent, E. H.; Scholes, G. D. Photovoltaic concepts inspired by coherence effects in photosynthetic systems. *Nat. Mater.* **2017**, *16*, 35−44.

(15) Hayes, D.; Griffin, G. B.; Engel, G. S. Engineering coherence among excited states in synthetic heterodimer systems. *Science* **2013**, *340*, 1431−1434.

(16) Wang, L.; Griffin, G. B.; Zhang, A.; Zhai, F.; Williams, N. E.; Jordan, R. F.; Engel, G. S. Controlling quantum-beating signals in 2D electronic spectra by packing synthetic heterodimers on single-walled carbon nanotubes. *Nat. Chem.* **2017**, *9*, 219−225.

(17) Caram, J. R.; Zheng, H.; Dahlberg, P. D.; Rolczynski, B. S.; Griffin, G. B.; Fidler, A. F.; Dolzhnikov, D. S.; Talapin, D. V.; Engel, G. S. Persistent Inter-Excitonic Quantum Coherence in CdSe Quantum Dots. *J. Phys. Chem. Lett.* **2014**, *5*, 196−204.

(18) Andrea Rozzi, C.; Maria Falke, S.; Spallanzani, N.; Rubio, A.; Molinari, E.; Brida, D.; Maiuri, M.; Cerullo, G.; Schramm, H.; Christoffers, J.; Lienau, C.; et al. Quantum coherence controls the charge separation in a prototypical artificial light-harvesting system. *Nat. Commun.* **2013**, *4*, 1602.

(19) Falke, S. M.; Rozzi, C. A.; Brida, D.; Lienau, C.; et al. Coherent ultrafast charge transfer in an organic photovoltaic blend. *Science* **2014**, *344*, 1001−1005.

(20) Song, Y.; Clafton, S. N.; Pensack, R. D.; Kee, T. W.; Scholes, G. D. Vibrational coherence probes the mechanism of ultrafast electron transfer in polymer-fullerene blends. *Nat. Commun.* **2014**, *5*, 4933.

(21) Pandya, R.; Chen, R. Y. S.; Cheminal, A.; Thomas, T.; Thampi, A.; Tanoh, A.; Richter, J.; Shivanna, R.; Deschler, F.; Schnedermann, C.; et al. Observation of Vibronic-Coupling-Mediated Energy Transfer in Light-Harvesting Nanotubes Stabilized in a Solid-State Matrix. *J. Phys. Chem. Lett.* **2018**, *9*, 5604−5611.

(22) Volpato, A.; Zerbetto, M.; Bolzonello, L.; Meneghin, E.; Fresch, B.; Benelli, T.; Giorgini, L.; Collini, E. Effect of Different Conformational Distributions on the Ultrafast Coherence Dynamics in Porphyrin-Based Polymers. *J. Phys. Chem. C* **2019**, *123*, 10212−10224.

(23) Hestand, N. J.; Spano, F. C. Expanded Theory of H- and J-Molecular Aggregates: The Effects of Vibronic Coupling and Intermolecular Charge Transfer. *Chem. Rev.* **2018**, *118*, 7069−7163.

(24) Würthner, F.; Saha-Möller, C. R.; Fimmel, B.; Ogi, S.; Leowanawat, P.; Schmidt, D. Perylene Bisimide Dye Assemblies as Archetype Functional Supramolecular Materials. *Chem. Rev.* **2016**, *116*, 962−1052.

(25) Huang, C.; Barlow, S.; Marder, S. R. Perylene-3,4,9,10-tetracarboxylic Acid Diimides: Synthesis, Physical Properties, and Use in Organic Electronics. *J. Org. Chem.* **2011**, *76*, 2386−2407.

(26) Lang, E.; Würthner, F.; Köhler, J. Photophysical Properties of a Tetraphenoxy-Substituted Perylene Bisimide Derivative Characterized by Single-Molecule Spectroscopy. *ChemPhysChem* **2005**, *6*, 935−941.

(27) Weil, T.; Vosch, T.; Hofkens, J.; Peneva, K.; Müllen, K. The Rylene Colorant Family—Tailored Nanoemitters for Photonics Research and Applications. *Angew. Chem., Int. Ed.* **2010**, *49*, 9068−9093.

(28) Serin, J. M.; Brousmiche, D. W.; Fréchet, J. M. J. Cascade energy transfer in a conformationally mobile multichromophoric dendrimer. *Chem. Commun.* **2002**, 2605−2607.

(29) Spenst, P.; Young, R. M.; Wasielewski, M. R.; Wuerthner, F. Guest and solvent modulated photo-driven charge separation and triplet generation in a perylene bisimide cyclophane. *Chem. Sci.* **2016**, *7*, 5428−5434.

(30) Eaton, S. W.; Shoer, L. E.; Karlen, S. D.; Dyar, S. M.; Margulies, E. A.; Veldkamp, B. S.; Ramanan, C.; Hartzler, D. A.; Savikhin, S.; Marks, T. J.; et al. Singlet Exciton Fission in Polycrystalline Thin Films of a Slip-Stacked Perylenediimide. *J. Am. Chem. Soc.* **2013**, *135*, 14701−14712.

(31) Angadi, M. A.; Gosztola, D.; Wasielewski, M. R. Organic light emitting diodes using poly(phenylenevinylene) doped with perylene-diimide electron acceptors. *Mater. Sci. Eng., B* **1999**, *63*, 191−194.

(32) Zhan, X.; Facchetti, A.; Barlow, S.; Marks, T. J.; Ratner, M. A.; Wasielewski, M. R.; Marder, S. R. Rylene and Related Diimides for Organic Electronics. *Adv. Mater.* **2011**, *23*, 268−284.

(33) Rybtchinski, B.; Sinks, L. E.; Wasielewski, M. R. Combining Light-Harvesting and Charge Separation in a Self-Assembled Artificial Photosynthetic System Based on Perylenediimide Chromophores. *J. Am. Chem. Soc.* **2004**, *126*, 12268−12269.

(34) Zhang, J.; Li, Y.; Huang, J.; Hu, H.; Zhang, G.; Ma, T.; Chow, P. C. Y.; Ade, H.; Pan, D.; Yan, H. Ring-Fusion of Perylene Diimide Acceptor Enabling Efficient Nonfullerene Organic Solar Cells with a Small Voltage Loss. *J. Am. Chem. Soc.* **2017**, *139*, 16092−16095.

(35) Bialas, D.; Bruning, C.; Schlosser, F.; Fimmel, B.; Thein, J.; Engel, V.; Wurthner, F. Exciton-Vibrational Couplings in Homo- and Heterodimer Stacks of Perylene Bisimide Dyes within Cyclophanes: Studies on Absorption Properties and Theoretical Analysis. *Chem. - Eur. J.* **2016**, *22*, 15011−15018.

(36) Wu, Y.; Young, R. M.; Frasconi, M.; Schneebeli, S. T.; Spenst, P.; Gardner, D. M.; Brown, K. E.; Wurthner, F.; Stoddart, J. F.; Wasielewski, M. R. Ultrafast Photoinduced Symmetry-Breaking Charge Separation and Electron Sharing in Perylenediimide Molecular Triangles. *J. Am. Chem. Soc.* **2015**, *137*, 13236−13239.

(37) Spenst, P.; Young, R. M.; Phelan, B. T.; Keller, M.; Dostal, J.; Brixner, T.; Wasielewski, M. R.; Wurthner, F. Solvent-Templated Folding of Perylene Bisimide Macrocycles into Coiled Double-String

DOI: 10.1021/acs.jpclett.9b02923
J. Phys. Chem. Lett. 2019, 10, 7498−7504

Ropes with Solvent-Sensitive Optical Signatures. *J. Am. Chem. Soc.* **2017**, *139*, 2014−2021.
(38) Spano, F. C. Spectral signatures of Frenkel polarons in H and J aggregates. *Acc. Chem. Res.* **2010**, *43*, 429−439.
(39) Cho, M. Coherent Two-Dimensional Optical Spectroscopy. *Chem. Rev.* **2008**, *108*, 1331−1418.
(40) Fuller, F. D.; Ogilvie, J. P. Experimental implementations of two-dimensional fourier transform electronic spectroscopy. *Annu. Rev. Phys. Chem.* **2015**, *66*, 667−690.
(41) Dean, J. C.; Scholes, G. D. Coherence Spectroscopy in the Condensed Phase: Insights into Molecular Structure, Environment, and Interactions. *Acc. Chem. Res.* **2017**, *50*, 2746−2755.
(42) Kukura, P.; McCamant, D. W.; Mathies, R. A. Femtosecond Stimulated Raman Spectroscopy. *Annu. Rev. Phys. Chem.* **2007**, *58*, 461−488.
(43) Frontiera, R. R.; Shim, S.; Mathies, R. A. Origin of negative and dispersive features in anti-Stokes and resonance femtosecond stimulated Raman spectroscopy. *J. Chem. Phys.* **2008**, *129*, 064507.
(44) Butkus, V.; Zigmantas, D.; Valkunas, L.; Abramavicius, D. Vibrational vs Electronic Coherences in 2DES. *Chem. Phys. Lett.* **2012**, *545*, 40−43.
(45) Turner, D. B.; Wilk, K. E.; Curmi, P. M. G.; Scholes, G. D. Comparison of Electronic and Vibrational Coherence Measured by Two-Dimensional Electronic Spectroscopy. *J. Phys. Chem. Lett.* **2011**, *2*, 1904−1911.
(46) Thyrhaug, E.; Tempelaar, R.; Alcocer, M. J. P.; Zidek, K.; Bina, D.; Knoester, J.; Jansen, T. L. C.; Zigmantas, D. Identification and characterization of diverse coherences in the Fenna-Matthews-Olson complex. *Nat. Chem.* **2018**, *10*, 780−786.
(47) Duan, H. G.; Prokhorenko, V. I.; Cogdell, R. J.; Ashraf, K.; Stevens, A. L.; Thorwart, M.; Miller, R. J. D. Nature does not rely on long-lived electronic quantum coherence for photosynthetic energy transfer. *Proc. Natl. Acad. Sci. U. S. A.* **2017**, *114*, 8493−8498.
(48) Chenu, A.; Christensson, N.; Kauffmann, H. F.; Mancal, T. Enhancement of vibronic and ground-state vibrational coherences in 2D spectra of photosynthetic complexes. *Sci. Rep.* **2013**, *3*, 2029.
(49) Son, M.; Park, K. H.; Yoon, M. C.; Kim, P.; Kim, D. Excited-State Vibrational Coherence in Perylene Bisimide Probed by Femtosecond Broadband Pump-Probe Spectroscopy. *J. Phys. Chem. A* **2015**, *119*, 6275−6282.
(50) Tekavec, P. F.; Myers, J. A.; Lewis, K. L. M.; Ogilvie, J. P. Two-dimensional electronic spectroscopy with a continuum probe. *Opt. Lett.* **2009**, *34*, 1390−1392.
(51) Hippius, C.; van Stokkum, I. H. M.; Zangrando, E.; Williams, R. M.; Wykes, M.; Beljonne, D.; Würthner, F. Ground- and Excited-State Pinched Cone Equilibria in Calix[4]arenes Bearing Two Perylene Bisimide Dyes. *J. Phys. Chem. C* **2008**, *112*, 14626−14638.
(52) Wu, Y.; Zhou, J.; Phelan, B. T.; Mauck, C. M.; Stoddart, J. F.; Young, R. M.; Wasielewski, M. R. Probing Distance Dependent Charge-Transfer Character in Excimers of Extended Viologen Cyclophanes Using Femtosecond Vibrational Spectroscopy. *J. Am. Chem. Soc.* **2017**, *139*, 14265−14276.

DOI: 10.1021/acs.jpclett.9b02923
J. Phys. Chem. Lett. 2019, 10, 7498−7504